AD_____

GRANT NUMBER DAMD17-94-J-4320

TITLE: Structure/Function of Recombinant Human Estrogen Receptor

PRINCIPAL INVESTIGATOR: Larry E. Vickery, Ph.D.

CONTRACTING ORGANIZATION: University of California
Irvine, California 92717

REPORT DATE: September 1997

TYPE OF REPORT: Annual

PREPARED FOR: U.S. Army Medical Research and Materiel Command
Fort Detrick, Maryland 21702-5012

REPORT DOCUMENTATION PAGE

Form Approved
OMB No. 0704-0188

1. AGENCY USE ONLY *(Leave blank)*	2. REPORT DATE	3. REPORT TYPE AND DATES COVERED
	September 1997	Annual (1 Sep 96 - 31 Aug 97)

4. TITLE AND SUBTITLE
Structure/Function of Recombinant Human Estrogen Receptor

5. FUNDING NUMBERS
DAMD17-94-J-4320

6. AUTHOR(S)
Larry E. Vickery, Ph.D.

7. PERFORMING ORGANIZATION NAME(S) AND ADDRESS(ES)
University of California
Irvine, California 92717

8. PERFORMING ORGANIZATION REPORT NUMBER

9. SPONSORING/MONITORING AGENCY NAME(S) AND ADDRESS(ES)
U.S. Army Medical Research and Materiel Command
Fort Detrick, Maryland 21702-5012

10. SPONSORING/MONITORING AGENCY REPORT NUMBER

11. SUPPLEMENTARY NOTES

12a. DISTRIBUTION / AVAILABILITY STATEMENT
Approved for public release; distribution unlimited

12b. DISTRIBUTION CODE

13. ABSTRACT *(Maximum 200*

Interaction of the estrogen receptor with its ligands is mediated by a C-terminal region of the protein designated the hormone binding domain (HBD). Extensive, unsuccessful, attempts were made to crystallize the protein. In the absence of structural data, we performed homology modeling of the HBD. One prediction of the model was the formation of an intrachain disulfide bond; however, no experimental evidence for the existence of the bond was found. The HBD did form disulfide bonds between peptides, supporting the prediction of either one or two surface exposed cysteine residues. Previous studies indicated that the dissociation of the HBD dimer in solution is a slow process with a half-life of ~1-2 hours, which ligand binding increased ~3-fold (estradiol) to ~4-fold (4-hydroxytamoxifen). HBD constructs with altered N-termini exhibited some differences in concentrations required for cooperativity and larger differences in dissociation half-life; others with only minor differences were found to be unstable. These results suggest that the N-terminus of the HBD contributes to folding of the protein and to dimer interactions.

14. SUBJECT TERMS	15. NUMBER OF PAGES
Breast Cancer	32
	16. PRICE CODE

17. SECURITY CLASSIFICATION OF REPORT	18. SECURITY CLASSIFICATION OF THIS PAGE	19. SECURITY CLASSIFICATION OF ABSTRACT	20. LIMITATION OF ABSTRACT
Unclassified	Unclassified	Unclassified	Unlimited

FOREWORD

Opinions, interpretations, conclusions and recommendations are those of the author and are not necessarily endorsed by the U.S. Army.

____ Where copyrighted material is quoted, permission has been obtained to use such material.

____ Where material from documents designated for limited distribution is quoted, permission has been obtained to use the material.

LW Citations of commercial organizations and trade names in this report do not constitute an official Department of Army endorsement or approval of the products or services of these organizations.

____ In conducting research using animals, the investigator(s) adhered to the "Guide for the Care and Use of Laboratory Animals," prepared by the Committee on Care and Use of Laboratory Animals of the Institute of Laboratory Resources, National Research Council (NIH Publication No. 86-23, Revised 1985).

____ For the protection of human subjects, the investigator(s) adhered to policies of applicable Federal Law 45 CFR 46.

LW In conducting research utilizing recombinant DNA technology, the investigator(s) adhered to current guidelines promulgated by the National Institutes of Health.

LW In the conduct of research utilizing recombinant DNA, the investigator(s) adhered to the NIH Guidelines for Research Involving Recombinant DNA Molecules.

____ In the conduct of research involving hazardous organisms, the investigator(s) adhered to the CDC-NIH Guide for Biosafety in Microbiological and Biomedical Laboratories.

Gary E Vodry 9-29-97

PI - Signature Date

Table of Contents

INTRODUCTION

The estrogen receptors are nuclear proteins evolutionarily-related to the receptors for the other steroid hormones, for vitamins A and D, and for thyroid hormone (1,2). The binding of ligands to these receptors is the initial step in a complex series of events culminating in an interaction of the ligand-bound receptor with the transcription machinery and modulation of gene expression. These receptor proteins exhibit four distinct properties required to exert their actions: hormone binding, multimeric complex formation, sequence specific DNA binding, and transcriptional modulation. The currently proposed schematic structure of these receptor proteins (shown in Figure 1 for the product of the estrogen receptor-α gene), based on sequence similarities and deletion analyses (summarized in reference 2), suggests that these proteins fold into at least three separate structural and functional domains: (i) an N-terminal domain having a highly variable length and amino acid sequence and believed to mediate much of the transcriptional enhancement activity of the protein, (ii) a highly conserved central domain of ~80 amino acids involved in DNA-binding, and (iii) a less well conserved C-terminal domain of ~250 amino acids that is involved in ligand binding.

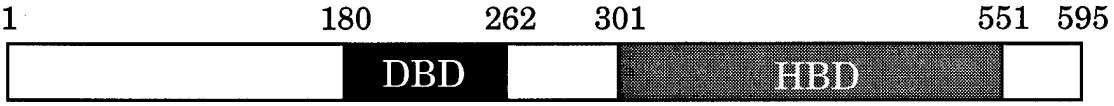

Figure 1. Schematic structure of the estrogen receptor-α. The locations of the N-terminal domain, DNA-binding Domain, and Hormone Binding Domain are shown using the amino acid numbering for the human protein.

The C-terminal hormone binding domain (HBD) is thought to contain many of the regulatory functions of the protein. Chimeric constructs containing fusions of fragments of the estrogen receptor with unrelated proteins such as the *myc* oncogene product, for example, display hormonal regulation of the activity of the fused gene products (3). This suggests that, even when removed from its normal environment, the HBD is not only capable of specific ligand binding, but may also retain the capacity to undergo the conformational changes that normally regulate the function of the receptor. Furthermore, the finding that the HBD can affect the activity of unrelated proteins suggests that the ligand-induced alteration in conformation may be a fundamental change in structure. The structure of the estrogen receptor HBD has not yet been reported, but crystal structures of the HBD from the human retinoid-X-receptor (RXR-α), human retinoic acid receptor (RAR-γ), and rat thyroid hormone receptor (TR-α) have recently been solved (4-6). Comparison of the ligand-free RXR-α and the ligand-bound RAR-γ structures led to the suggestion that ligand binding to the nuclear-receptor family proteins alters the conformation of the C-terminus of the HBD, a region previously proposed to contain a conserved transcriptional activation function (7,8).

The nuclear receptor superfamily proteins form dimers. This property has at least two functional roles: most of the proteins in the family are thought to bind DNA as dimers, and dimer formation allows cooperative ligand binding, thereby narrowing the ligand concentration range required for full biological effect. The nature of the dimer interface of the full-length receptor protein is not established. The isolated DNA-binding domain has been shown to dimerize in the presence of DNA, suggesting that some of the dimerization interface resides within this portion of the protein; the isolated DNA-binding domain, however, is monomeric in solution. The HBD is also thought to play a role in dimerization. We have shown that the isolate estrogen receptor HBD forms dimers in solution (see 1996 progress report and ref. 9). However, the regions of the HBD that are involved in dimerization have not yet been fully mapped, and the role dimerization plays in the function of the protein has not yet been established.

Recently a second gene, designated estrogen receptor-β, was discovered in several mammalian species (10), including humans (11). The product of this gene is smaller than the estrogen receptor-α (477 versus 595 amino acids). The DNA binding domains of the two proteins exhibit a high degree of sequence similarity (~95%), while the hormone binding domain is fairly similar (~60% identity); the remainder of the proteins are quite divergent. Unless otherwise noted, all of the discussion included in this progress report refers to the estrogen receptor-α.

Current progress includes a series of unsuccessful crystallization attempts, analysis of the role of the N-terminus of the HBD in folding and dimer interactions, and analysis of cysteine exposure in the folded protein to test a theoretical model of the protein.

List of abbreviations

The abbreviations used are: AEBSF, [4-(2-aminoethyl)-benzenesulfonylfluoride]; CD, circular dichroism; DEAE, diethylaminoethyl; DTT, dithiothreitol; DTNB, 5, 5′-dithio-bis-(2-nitrobenzoic acid); HBD, hormone binding domain; MBP, maltose-binding protein; RAR, retinoic acid receptor, RXR, retinoid-X-receptor; TED, Tris-EDTA-DTT, TNB, thio-2-nitrobenzoic acid; TR, thyroid hormone receptor.

MATERIALS AND METHODS

Supplies – Restriction endonucleases and other enzymes used for DNA manipulation were obtained from Boehringer-Mannheim Corp. (Indianapolis, IN), New England Biolabs, Inc. (Beverly, MA), Stratagene Cloning Systems (La Jolla, CA), or United States Biochemical Corp. (Cleveland, OH). Synthetic oligonucleotides were obtained from Operon Technologies (Alameda, CA) or Genosys Biotechnologies, Inc. (The Woodlands, TX). Bacterial growth media components were purchased from Difco (Detroit, MI); other reagents were obtained from Sigma Chemical Company (St. Louis, MO). Tritiated estradiol was obtained from Amersham and New England Nuclear. The estrogen antagonist *trans*-4-hydroxytamoxifen was a gift from Dr. Dominique Salin-Drouin (Laboratories Besins-Iscovesco) and ICI 182,780 was a gift from Dr. Alan Wakeling (ICI Pharmaceuticals).

Vector Construction – Unless otherwise noted, all DNA manipulations were carried out by standard techniques (13). As described in the previous progress reports, a DNA fragment coding for the human estrogen receptor hormone binding domain (amino acids 301-551) was generated by PCR from the HE0 estrogen receptor-α cDNA plasmid (14). The PCR fragment was digested with *Eco*RI and subcloned into the pMAL-c2 vector (New England Biolabs) which had been digested with *Xmn* I and *Eco*RI. Following isolation of the insert-containing plasmid, the entire HBD coding region was sequenced to confirm the absence of errors introduced by PCR amplification. The presence of the cDNA mutation Gly400Val (15) was verified by DNA sequencing; this mutation was reverted to wild-type using a PCR mutagenesis procedure (16), creating the plasmid pER08 (the Appendix contains a list of plasmids and their designations).

Protein products of pMAL-c2 derived plasmids consist of the maltose binding protein fused to the desired protein with a linker peptide consisting of $(Asn)_{10}$-Leu-Gly-Ile-Glu-Gly-Arg; the terminal four residues of the peptide comprise a Factor X_a cleavage signal. Factor X_a hydrolysis of the expressed fusion protein, however, resulted in heterogeneous, largely inactive peptides; we therefore modified the linker region to generate the sequence Asn-Gly, which can be cleaved by hydroxylamine (17). Bases encoding residues Leu-Gly-Ile-Glu of the Factor X_a recognition sequence were mutated to Asn codons by site-directed mutagenesis using the unique site-elimination procedure (18) with the Transformer kit from Clontech (Palo Alto, CA). The coding region of the mutagenesis product was sequenced; the modified DNA was found to encode a linker peptide of $(Asn)_{14}$-Gly-Arg. This plasmid was designated pER304. Unique site-elimination was then performed on pER304 to mutate Ser-305 to Glu, creating pER336. The product of hydroxylamine cleavage of the fusion protein from pER304, pER336, and a number of constructs derived from these plasmids retains Gly-Arg from the linker, the latter of which corresponds to the naturally occurring Arg-300.

Plasmids beginning at sites other than position 300 were constructed by subcloning PCR products into pMAL-c2, or into pMAL-INGR (pMAL-c2 in which the Glu from the Factor X_a site was mutated to Asn) in a manner similar to that described for pER08. Other plasmids discussed were constructed by site-directed

mutagenesis of previously existing plasmids containing appropriate characteristics.

Protein Expression and Purification – Competent TOPP2 cells (Stratagene) were transformed with the expression plasmids. Cells containing the appropriate plasmid were grown in TB media in the presence of 100 μg/ml ampicillin to an OD_{600} of ~1.7; protein expression was induced by the addition of IPTG to a final concentration of 0.25 mM and cultures were grown overnight at ambient temperature (usually ~27 °C).

The cells were harvested by centrifugation and frozen overnight at -20 °C. The cell pellets were resuspended in lysis buffer (50 mM Tris-HCl, 10 mM EDTA, 2 mM DTT, 1 mM AEBSF (Cal Biochem), pH 8.0, and 1 mg lysozyme/g of cells). After ~1 hr at ambient temperature, $MgCl_2$ was added to a final concentration of 120 mM and the lysate treated with DNase and RNase. The supernatant from a 40,000 x g centrifugation of the lysate was diluted 3-fold in TED buffer (20 mM Tris-HCl, 1 mM EDTA, and 1 mM DTT, pH 7.3) and applied to a DEAE-cellulose column (Whatman). The flowthrough from the DEAE-cellulose column was applied to an amylose resin column (New England Biolabs). After washing with 2-4 column volumes of TED containing 0.2 M NaCl, the fusion protein was eluted with 10 mM maltose in the same buffer.

The eluted protein was diluted 5-fold and applied to a DEAE-Sepharose column (Pharmacia). This column was washed with 5 column volumes of TED containing 0.05 M NaCl, and the protein was eluted with either a linear NaCl gradient (0.05-0.2 M NaCl; the fusion protein eluted at 0.13-0.16 M NaCl) or with 0.15 M NaCl in TED buffer. The fusion protein was then concentrated to ~20 mg/ml by precipitation with 60% ammonium sulfate or ultrafiltration (Amicon Centriprep) and was digested for 60-72 hours at ambient temperature with hydroxylamine (final concentration: 2 M hydroxylamine-HCl, 0.2 M Tris-HCl, pH 9.0). The cleaved HBD peptide was separated from the maltose binding protein by Sephadex G-100 gel filtration chromatography.

The final preparation of the purified pER304 or pER336-derived HBD peptide was stable and could be stored at 4 °C or -70 °C for several months. Some of the other constructs yielded unstable proteins (see subsequent sections).

Spectroscopy – All spectroscopy was performed at ambient temperature. Absorbance spectra were obtained using a Cary 1 spectrophotometer calibrated with $K_3Fe(CN)_6$ assuming ε_{420} = 1,020 $(M \cdot cm)^{-1}$. The concentration of purified MBP-HBD fusion protein and of isolated HBD peptide were determined spectrophotometrically assuming ε_{280} = 89,365 $(M \cdot cm)^{-1}$ for the fusion protein and 23,745 $(M \cdot cm)^{-1}$ for the HBD peptide; these values are based on a composition of 11 tryptophan and 20 tyrosine residues (fusion protein) or 3 tryptophan and 5 tyrosine residues (HBD peptide) predicted from the cDNA sequence and on average extinction coefficients for tryptophan (5615 $(M \cdot cm)^{-1}$) and tyrosine (1380 $(M \cdot cm)^{-1}$) (19,20). For the tryptophan mutants, the altered extinction coefficients were taken into account while determining concentrations.

Analytical Gel Filtration – The apparent molecular weight of the fusion protein

and HBD were determined using a Pharmacia FPLC system and a Superdex 200 HR 10/30 gel filtration column (running buffer 20 mM Tris-HCl, 1 mM EDTA, 200 mM NaCl, pH 7.3). The column was calibrated using blue dextran to determine the void volume and with the following standard proteins: thyroglobulin (669 kDa), ferretin (440 kDa), catalase (232 kDa), aldolase (158 kDa), bovine serum albumin (69 kDa), ascorbate peroxidase (57.5 kDa), P450eryF (45.8 kDa), ovalbumin (43 kDa), MBP (40.4 kDa), rhodanese (33.3 kDa), chymotrypsinogen (25 kDa), ribonuclease A (13.7 kDa), and cytochrome c (12.4 kDa).

For the kinetic experiments, equimolar amounts of the fusion protein and HBD peptide were mixed and incubated at ambient temperature (~25°C). At various times aliquots were taken and subjected to FPLC gel filtration. For the experiments in the presence of ligand, the column was pre-equilibrated in the same running buffer with 50 nM of the relevant ligand, and 2 μM solutions of each protein pre-equilibrated overnight with 5 μM of the ligand. The integrated peak areas were corrected for extinction coefficient of the relevant protein species to determine the concentration of each species (*i.e.* fusion homodimer, HBD homodimer, or heterodimer) present at the time of injection (the relative amount of each species was assumed not to change during the chromatography). For experiments in the presence of ligand, the extinction coefficient of the protein was corrected for contributions of the bound ligand (assumed to be ~2,000 $(M \cdot cm)^{-1}$ for estradiol and ~15,000 $(M \cdot cm)^{-1}$ for 4-hydroxytamoxifen).

The rate constant for dissociation, k, was determined by least-squares non-linear regression of the first order rate equation:

$$D_t = (D_0 - D_f)e^{-kt} + D_f$$

where D_t is the concentration of one homodimer at time t, D_0 is the initial concentration of homodimer, and D_f is the final concentration of homodimer after the rearrangement had gone to completion. Half-life ($t_{1/2}$) for dissociation is defined as $\ln(2)/k$.

Free Cysteine Determination – The HBD peptide was diluted into phosphate buffer (0.1 M potassium phosphate, 1 mM EDTA, pH 7.25); added excess 5, 5′-dithio-bis(2-nitrobenzoic acid) (DTNB). In the presence of free sulfhydryl groups, DTNB covalently modifies the sulfhydryl and releases thionitrobenzoic acid (TNB). This results in a $\Delta\varepsilon_{412}$ of 14,000 $(M \cdot cm)^{-1}$.

Radioreceptor Assay – The HBD peptide was incubated overnight with various concentrations of [6,7-^{3}H]-estradiol at 4 °C in TED buffer including 0.2 M NaCl and 1 mg/ml porcine gelatin; bound and unbound steroids were separated using dextran-coated charcoal (0.625% charcoal, 0.125% dextran) in the same buffer without gelatin. In all experiments using purified and partially purified protein, the binding of radioactive estradiol in the presence of a 100-fold excess of unlabeled estradiol was equivalent to the non-specific binding observed in the absence of any added HBD protein. The presence of a carrier protein in both the ligand and protein buffers was found to be necessary to obtain reproducible results; porcine gelatin (1 mg/ml), bovine γ-globulin (4 mg/ml), or bovine serum albumin (4 mg/ml) gave

similar results.

In some cases, Scatchard plots (24) are shown for clarity; however, the data for bound and free steroid were directly fitted to the Hill equation (25):

$$[B] = \frac{B_{max}[F]^n}{(F_{0.5})^n + [F]^n}$$

using least squares non-linear regression analysis to estimate the $F_{0.5}$ (or K_d when n = 1), B_{max}, and n (Hill coefficient).

RESULTS AND DISCUSSION

Crystallization Attempts

One of the major goals of this project is to obtain structural information for the HBD using X-ray crystallographic analysis; this would be particularly useful for rational drug design. In order to determine the structure of the protein using this method, it is necessary to produce large amounts of homogeneous protein and to find conditions under which the protein will crystallize. The first of these goals has been met; the second has proven rather difficult. Several hundred milligrams of a number of different fusion proteins have been produced and apparently homogeneous cleavage of several of these in large quantities has been achieved.

In order for proteins to crystallize their tendency to remain in the solution must be lower than their concentration in the solution. However, if this disparity is too great, the protein will aggregate and precipitate in a non-ordered fashion. It is therefore necessary to find conditions where the protein will leave the solution in an orderly manner. In attempting to find these conditions, we have screened several thousand different buffer, precipitant, and ionic strength, and pH conditions using both fusion proteins and HBD peptides for several different mutants.

The HBD peptides are hydrophobic, and have a marked tendency to aggregate. A number of constructs are soluble at 15-20 mg/ml when treated gently. The majority of these have been tested for crystallization. We have not yet found conditions under which any of these constructs form crystals.

An alternative approach has been to use the MBP-HBD fusion protein, since the more hydrophilic fusion protein has a lower tendency to form non-specific aggregates. The MBP has been crystallized, suggesting that the presence of this additional peptide may contribute useful intermolecular contacts during the crystallization process. In addition, the fact that the structure of the MBP is known would simplify analysis of the diffraction data. Thus far, however, none of the fusion protein constructs have formed crystals.

One possible reason for the limited success with the fusion protein is that the linker peptide that connects the MBP and HBD is too flexible, and as a result, it allows the fusion protein to adopt too many conformations in solution. Based on this suggestion, we are in the process of producing constructs that contain much shorter linker peptides (varying from 3 to 7 amino acids, instead of 18 amino acids), which may form less flexible proteins with greater probability of forming ordered crystals.

A variety of other expression plasmids have been constructed (see subsequent sections); as protein becomes available, these will be tested for crystal formation.

Molecular modeling

Our understanding of the function of the estrogen receptor would be greatly

enhanced by three-dimensional structural information. In the absence of crystallography data for this protein, we used the known structure of the related (~25% sequence identity) RXR-α HBD to generate a model for the estrogen receptor HBD for both ER-α and ER-β. It must be emphasized that the results of this procedure are only a model with a potentially limited relationship to reality; on the other hand, this model does allow interpretation of some of the results obtained, and has suggested additional experimental directions.

Manuel Peitsch has set up a computer server (http://expasy.hcuge.ch/swissmod/SWISS-MODEL.html, see ref. 26-28) which allows the entry of a protein sequence; the computer then models this protein based on previously solved structures. Currently, only the RXR-α structure is available for modeling the estrogen receptor HBD.

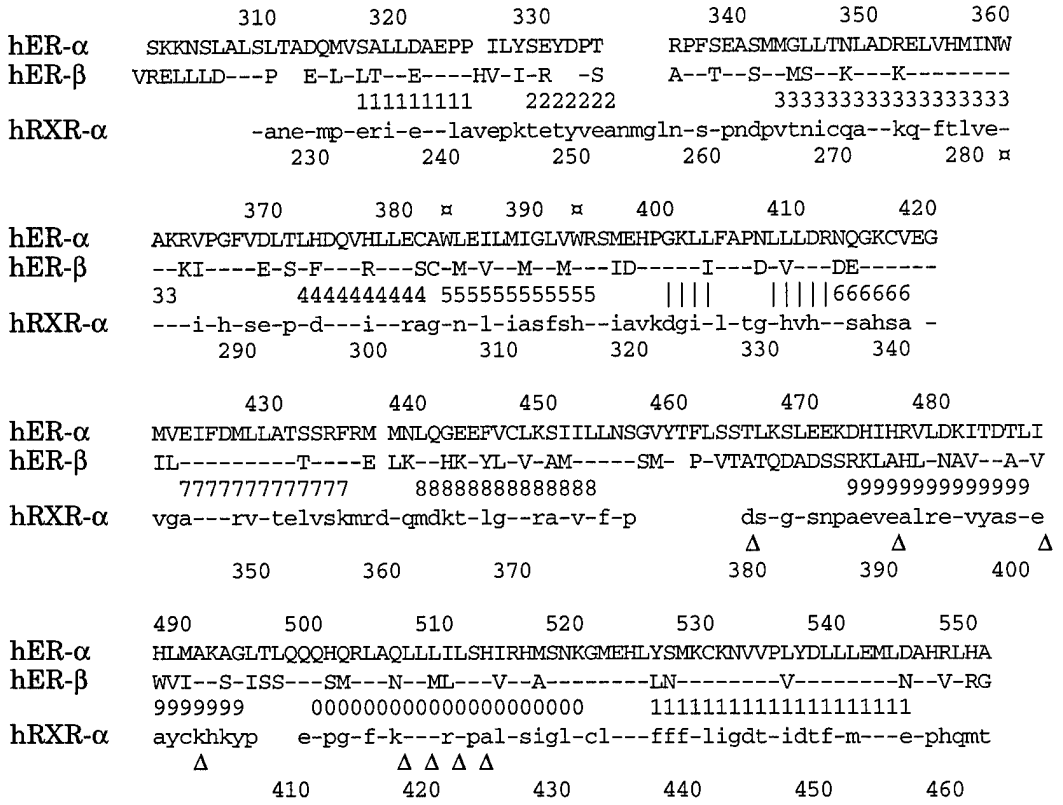

Figure 2. Sequence alignment of the HBD for the human estrogen receptor-α and β with human RXR-α. Dashes indicate identities with the ER-α sequence. The numbers between the sequences show the locations of the α-helices in the RXR structure; the vertical lines indicate the β-sheet in the RXR. The ¤ symbols indicate the three ER-α HBD tryptophan residues (note that Trp-393 is not conserved in the RXR sequence). The Δ symbols indicate important dimer contacts in the RXR structure.

The initial model is energy minimized by the server computer. Examination of the initial model and of the sequence alignment generated by the computer revealed

a number of regions that were unlikely to be modeled correctly; the program allows additional steps using sequence alignments generated by the investigator. The alignment we used for the final models is shown in Figure 2. The alignment (*i.e.* the precise location of the gaps introduced) is slightly different from that based entirely on sequence identity.

The major assumption that underlies the homology modeling procedure is that related proteins have similar overall folds. The resulting ER model therefore looks very similar to the RXR structure, exhibiting ~60% α-helix, and a small β-sheet, with only the inter-helix loops having different structures. Because ER residue Ser309 aligns with the first visible residue of the RXR, this is the first residue of the ER HBD model.

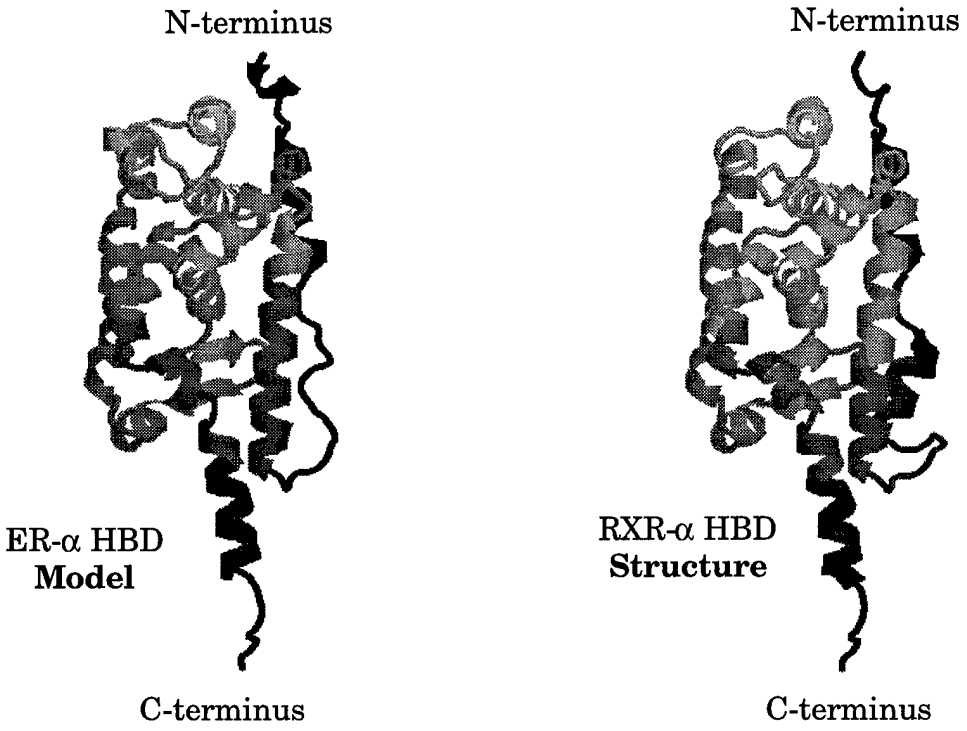

Figure 3. Comparison of the predicted ER HBD model to the RXR crystal structure.

The current theoretical understanding of protein structure is too limited to allow us to state unambiguously how close this generated model is to the actual structure. Some features, however, suggest that this model is at least physically consistent. The RXR-α structure contains several buried or largely buried salt bridges. All of these appear to be conserved in the model (Table 1) In addition, there is a buried salt bridge in the model (ER-α: Glu353–Lys531; ER-β: Glu252-Lys429) not present in the RXR-α structure. These residues are adjacent to conserved sequences but are widely separated in the primary sequence of the protein; the presence of the two charged residues in both ER-α and ER-β where none exist in the RXR-α sequence suggest that this additional buried salt bridge may actually exist. The alignment used was based on this type of analysis; other alignments with

slightly greater numbers of identical residues resulted in buried charged residues without compensating charges of opposite signs, or in disruption of some of the buried salt bridges listed in Table 1.

Table 1
Buried Charged Residues in the RXR-α Structure and in the ER HBD Models

RXR-α Structure	ER-α Model	ER-β Model
Glu239 – Arg371	Glu323 – Lys449	Glu223 – Lys348
Glu307 – Arg426	Glu385 – Arg515	Glu284 – Lys413
Glu366 – Arg414	Glu444 – Arg503	Glu343 – Arg401
—	Glu353 – Lys531	Glu252 – Lys429

Inspection of the model based on the wild-type estrogen receptor sequence revealed the presence of a disulfide bond between Cys381 and Cys530. If this disulfide bond were in fact present, the entrance to the predicted ligand binding would be sealed. In addition, Cys530 has been shown to be labelled by photoactivatible ligand analogs (29), suggesting that this residue does not normally form an intrachain disulfide bond. Furthermore, while Cys530 is conserved in the ER-β sequence, the residue that corresponds to Cys381 is a Ser in ER-β, and the modeling software does not predict disulfide formation for ER-β using a nearby Cys. It is possible, however, that the sub-stoichiometric ligand binding observed with some HBD peptide preparations may be due to formation of an intrachain Cys381-Cys530 disulfide bond. This possibility is discussed in more detail below.

Assuming that this disulfide is in fact an artifact of the modeling software, Cys530 and Cys381 were theoretically individually mutated to Ser and the modeling was repeated. These resulted in very similar models with no disulfide bonds predicted. The Cys530Ser mutant is the model that will be referred to periodically in subsequent sections. It should be emphasized that this estrogen receptor model is a model, and it may deviate widely from the correct structure.

Free Cysteine Determination

The estrogen receptor HBD has four Cys residues. The homology modeling software predicts that two of these form a disulfide bond. The position of this

putative disulfide makes this somewhat unlikely. As shown in Figure 4, this disulfide would interfere with entry of the ligand into the binding site.

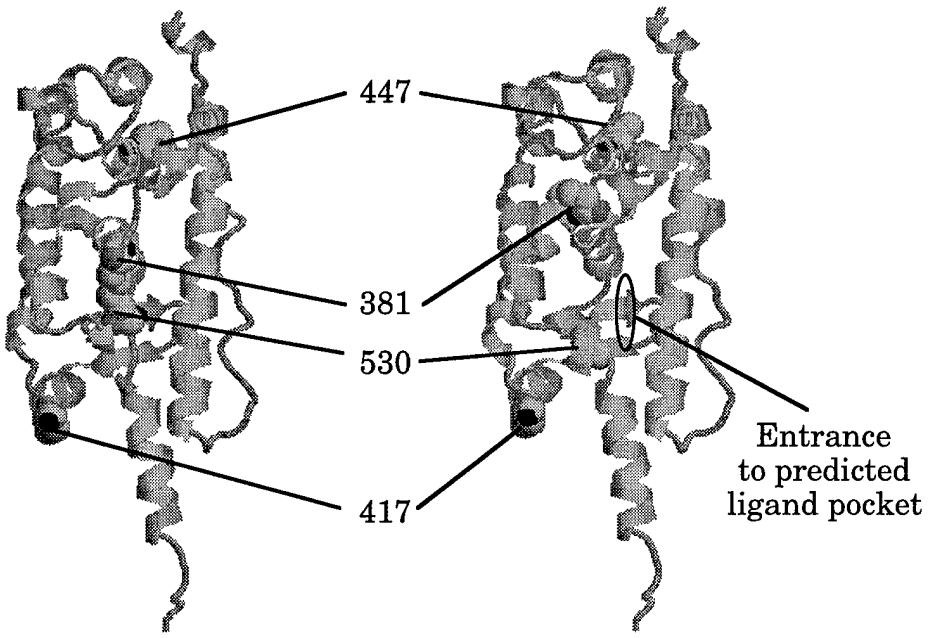

Figure 4. Position of cysteine residues in estrogen receptor models. The model on the left shows the Cys381–Cys530 disulfide bond predicted by the modeling software based on the wild-type sequence; the model on the right shows the results of the modeling with Cys530 theoretically mutated to Ser, and the location of the predicted ligand binding pocket.

To test whether the HBD peptide actually does undergo disulfide formation, a sample of the pER304 HBD peptide was stored in the absence of reducing agent. This would allow the formation of both the possible intrachain disulfide, and of interchain disulfide bonds.

An SDS polyacrylamide gel run on the HBD peptide stored both in the presence and absence of reducing agent (DTT). Each sample was run under both reducing and non-reducing conditions (Figure 5).

Based on the gel in Figure 5, it is clear that a significant amount of the HBD stored without DTT has formed interchain disulfide bonds. However, this may represent denatured protein. Aliquots of this sample were therefore subjected to size-exclusion chromatography before and after a brief incubation with excess DTT (Figure 6).

The results of the chromatogram suggest that the protein was not denatured. The major peak migrated at the size expected for an HBD dimer, with an additional peak at the size of a tetramer, and a shoulder at the size of a larger complex. Following incubation with DTT, nearly all of the HBD peptide migrated as a dimer. If the HBD were denatured, it would run as a monomer, and there is no evidence of a monomer in the chromatograms.

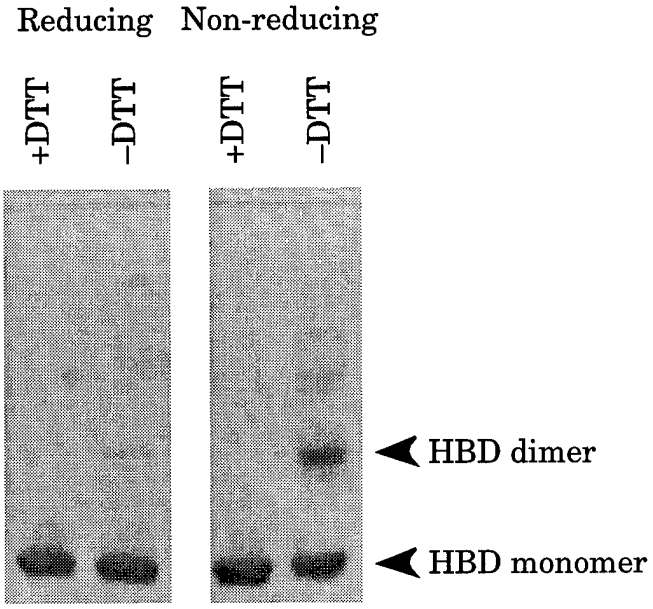

Figure 5. SDS PAGE run on HBD peptide stored in the presence and absence of DTT.; the samples were boiled in SDS sample buffer under reducing or non-reducing conditions. Note the presence of multimers that disappear under reducing conditions.

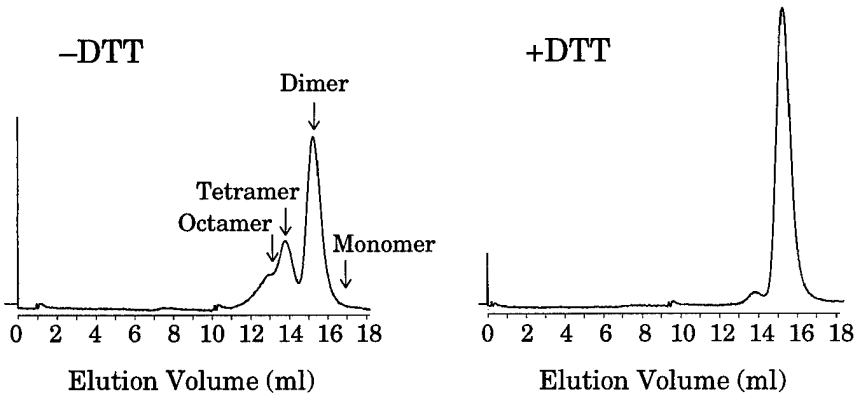

Figure 6. Superdex-200 size exclusion chromatograms of HBD peptide. The left panel shows an HBD sample stored in the absence of DTT, with arrows indicating the expected migration positions of different HBD complexes. Note the higher molecular weight peaks migrating at smaller elution volumes than the HBD dimer peak. Following a 1 hour incubation in the presence of excess DTT (right panel), essentially all of the HBD migrates as a dimer.

The number of exposed and total free cysteine residues was measured using DTNB. In the presence of a free sulfhydryl groups, DTNB releases TNB, resulting

in a marked increase in absorbance at 412 nm. The HBD was separated from the DTT used during the purification procedure by gel filtration. An aliquot of this HBD was incubated with DTNB at ~25°C; the absorbance spectrum suggested that between one and two cysteine residues were accessible. Heating the sample to 68°C resulted in the exposure of ~4 cysteine (Figure 7).

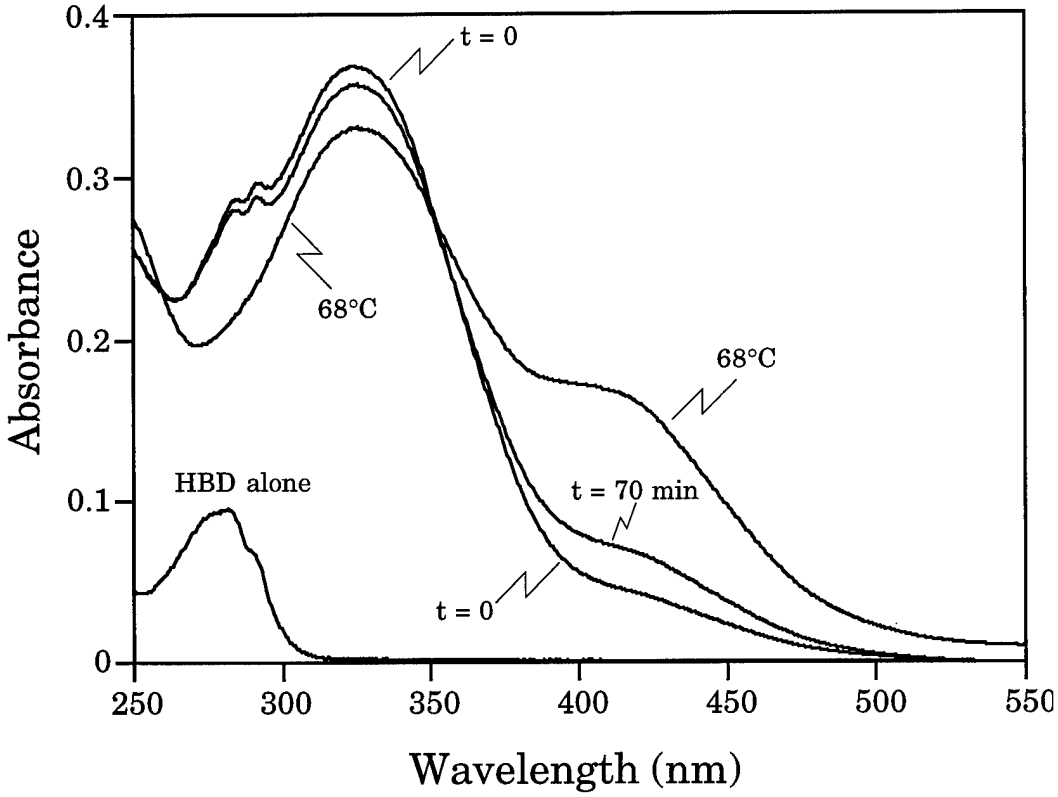

Figure 7. Absorbance spectra for HBD in the presence of DTNB. Absorbance spectra were measured prior to addition of DTNB, immediately after addition, following 70 minutes at 25°C, and after 5 minutes at 68°C. The change in absorbance at 412 nm is proportional to the number of free sulfhydryl groups present in the protein.

The sample of HBD stored in the absence of reducing agent was also tested for free cysteines using DTNB. With this sample, ~1 cysteine were found to be exposed, and a total of slightly more than 3 cysteine residues were found after denaturation of the protein.

The results presented in Table 2 suggest that one of the cysteine residues of the HBD is fully exposed on the surface, and one partially exposed. Of these, at least one is probably capable of forming interchain disulfide bonds; based on the model, this is probably Cys417, with Cys381 probably being partially exposed. The model predicts that Cys530 is largely buried, and Cys447 completely buried. We previously found that mutation of Cys447 to the more bulky Trp is unstable, which supports the prediction that this residue is buried.

Table 2
Free Cysteine Residues in HBD

Time after DTNB Addition	Apparent Number of Cysteines Labelled	
	HBD Stored in Presence of DTT	HBD Stored in Absence of DTT
0	1.0	0.5
25°C for 30 minutes	1.5	0.9
25°C for 60 minutes	1.7	1.0
68°C for 5 minutes	4.0	3.3

The estrogen binding was also measured for these HBD preparations. In these experiments, the binding stoichiometry of the protein stored in the presence and absence of DTT were similar (Figure 8). However, when the binding data were examined for several different concentrations of HBD peptide, it was observed that the HBD stored in the absence of DTT exhibited a smaller degree of positive cooperativity than that stored in the presence of DTT (Figure 9).

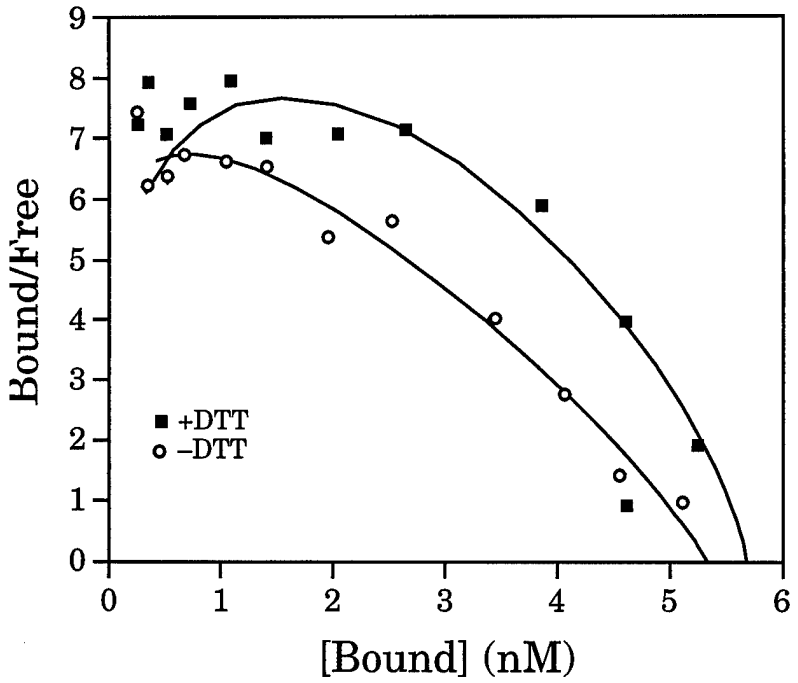

Figure 8. Scatchard plots for HBD peptides stored in the presence and absence of DTT. The assay used 5.6 nM of each protein. The Scatchard plot of the data for both samples exhibit the convex curvature indicative of positive cooperativity; the +DTT sample had a Hill coefficient of 1.38, while the –DTT sample had a Hill coefficient of 1.15.

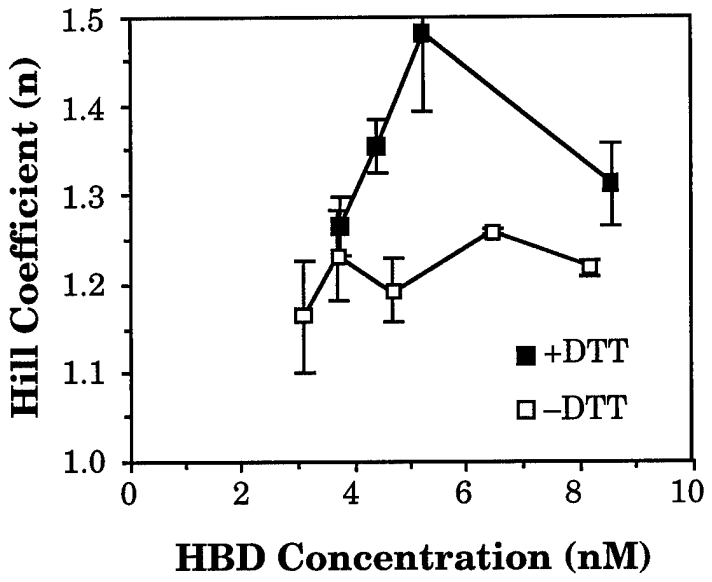

Figure 9. Variation of Hill coefficient with HBD concentration for peptides stored in the presence and absence of DTT. Each data point represents at least two separate determinations of the Hill coefficient.

Taken together, the results of the chromatography (Figure 6) and the DTNB (Figure 7) experiments suggest that the only disulfide bonds being formed are probably between separate chains, rather than within the chain as predicted by the modeling software. Identification of the cysteine residue or residues involved forming these bonds would act as a test of the model's predictions of Cys417 and Cys381 surface accessibility. The results of the binding assay suggest that these interchain bonds may interfere with the conformational changes required for cooperative estradiol binding. Since the binding affinity for estradiol is only slightly affected, and since the HBD is not denatured by the disulfide bond formation, it is likely that disulfide bonds between the chains does not result in major changes in the structure of the HBD.

Effect of Varying N-termini

One feature of peptides that may interfere with crystallization is disordered N- or C-termini; it is thus often useful to minimize the length of the peptide fragments expressed for crystallography. In addition, in previous experiments while attempting to generate fusion proteins that yielded homogeneous cleavage to form the HBD, we noted some alterations in behavior of the peptide dimers that appeared to correlate with sequence at the N-terminus. Finally, in the crystal structure of the RXR HBD, the N-termini appear in fairly close proximity (Figure 10), suggesting that they may affect dimerization. Since the ER-α and ER-β are thought to form heterodimers, the sequence of the N-terminus of the HBD may assist in controlling the strength and specificity of this interaction.

Protein was expressed from plasmids containing several different HBD coding sequences. Figure 11 shows the junction between the MBP and the HBD for these constructs (the designation, given to the left of each protein sequence in Figure 11, refers to our code number for the plasmids).

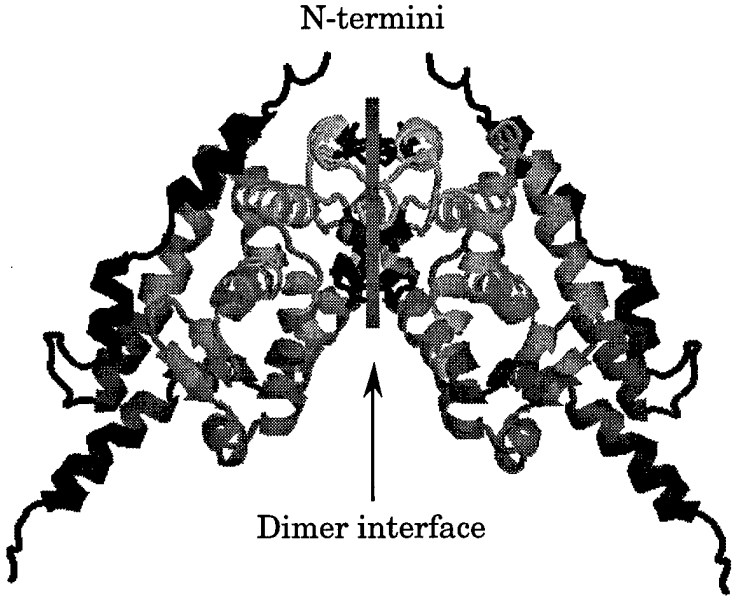

Figure 10. The RXR HBD dimer structure. Although the residues that comprise the dimer interface are toward the C-terminus of the protein sequence (helices 9 and 10; residues ~400-425 of the RXR), the interface is in close proximity to the N-terminus in the three dimensional structure.

The constructs shown in Figure 11 are shown from longest to shortest. Each HBD peptide has a Gly as the N-terminal residue following cleavage with hydroxylamine. The peptides were evaluated for stability, for estrogen binding and cooperativity, and for dimer dissociation kinetics.

The first construct, pER304, contains two cleavage sites for hydroxylamine, the intended one (shown with the vertical line in Figure 11), and a second one between Asn304 and Ser305. The HBD produced from the cleavage reaction contains roughly 20% of the shorter peptide; it is otherwise stable.

In examining the structural model, it appears that Ser309 corresponds to Ser225 of the RXR (the first residue reportedly visible in the electron density map). Note, however, the gaps that had to introduced before ER Arg335 (see Figure 2); it is therefore possible that the ER HBD begins at about Ser305. On the other hand, the N-terminal residues of the RXR do not appear to interact strongly with the core of the HBD, so shorter constructs might be predicted to be stable. The pER330 gene product (four residues shorter than pER304) is stable, as is pER335 (two residues shorter than pER330). However, pER349, three residues shorter than pER335, exhibits only limited stability; the fusion protein has a marked tendency to aggregate and precipitate during purification. The shorter constructs, pER338 and

pER337 were found to be unstable, with minimal activity, and essentially all of the protein denatured during purification. These results suggest that the HBD probably begins between 307 and 309. However, it should be noted that in all of these cases there are several mutations introduced both by the residues that remain in these constructs after cleavage and by the residues of the MBP and linker (which may affect stability of the HBD portion of the fusion protein).

```
                                    300       310       320       551
                                     *         *         *         *
pER304   MBP ... NSSSNNNNNNNNNNNNNN|GRSKKNSLALSLTADQMVSALLD . . . 551
                                        + ++        -       -

                                    300       310       320       551
                                     *         *         *         *
pER336   MBP ... NSSSNNNNNNNNNNNNNN|GRSKKNELALSLTADQMVSALLD . . . 551
                                        + ++ -      -       -

                                    300       310       320       551
                                     *         *         *         *
pER348   MBP ... NSSSNNNNNNNNNNNNNN|GRSKKDELALSLTADQMVSALLD . . . 551
                                        + ++--      -       -

                                   305  310       320       551
                                     *    *         *         *
pER330      MBP ... NSSSNNNNNNNNNNLGIN|GRSLALSLTADQMVSALLD . . . 551
                                          +       -       -

                                   305  310       320       551
                                     *    *         *         *
pER345      MBP ... NSSSNNNNNNNNNNLGIN|GESLALSLTADQMVSALLD . . . 551
                                          -       -       -

                                         310       320       551
                                          *         *         *
pER335   MBP ... GSSSNNNNNNNNNNLGIEGRSKKN|GLALSLTADQMVSALLD . . . 551
                                                  -       -

                                         310       320       551
                                          *         *         *
pER349         MBP ... NSSSNNNNNNNNNNLGIN|GRLTADQMVSALLD . . . 551
                                            +   -       -

                                        312       320       551
                                         *         *         *
pER338       MBP ... NSSSNNNNNNNNNNLGINGRSKKN|GADQMVSALLD . . . 551
                                                  -       -

                                           315  320       551
                                            *    *         *
pER337            MBP ... NSSSNNNNNNNNNNLGIN|GRMVSALLD . . . 551
                                                +       -
```

Figure 11. HBD peptides with differing N-termini. Each is expressed as an MBP fusion protein. The intended cleavage sites are shown with a vertical line; the sequence to the right of the line is included in the HBD peptide. Mutations (*i.e.* residues not part of the wild-type HBD sequence) are shown in bold. Charged residues retained in the HBD sequence following cleavage are indicated by (+) or (–).

Other constructs also suggest that the N-terminus of the HBD is important. The sole difference between pER330 and pER345 is the mutation of the Arg (the second residue after the cleavage site) to Glu. This charge reversal mutation (at the same site as the introduced Asp in pER348) results in an unstable protein. While pER336 and pER348 with one or two additional negative charges, respectively, are stable, pER345 (which lacks the basic residues at the extreme N-terminus of the HBD) is not. These results suggest that positively charged residues near the N-terminus of the HBD are required for stability of the HBD.

As was described in the previous progress reports, cooperative estradiol binding is observed for the HBD peptides at higher peptide concentrations (see, for example, the data shown in Figure 8), while at peptide concentrations below ~1-2 nM non-cooperative binding is observed. All of the constructs sufficiently stable to be purified and cleaved (*i.e.* all listed in Figure 11 except pER337, pER338, and pER345) exhibited high affinity estradiol binding with similar affinities. These peptides also exhibited positive cooperativity with similar maximal Hill coefficients (Table 3), with the possible exception of pER335, which seems to have a slightly higher maximal cooperativity.

Table 3
Estradiol Binding by HBD N-terminal Mutant Peptides

HBD Peptide	K_d for Estradiol (nM) (*i.e.* $F_{0.5}$ at n = 1.0)	Maximal Hill Coefficient
pER304	0.39 ± 0.20	1.46 ± 0.08
pER336	0.17 ± 0.06	1.46 ± 0.09
pER348	0.17 ± 0.06	1.43 ± 0.08
pER330	0.33 ± 0.09	1.44 ± 0.03
pER335	0.24 ± 0.16	1.77 ± 0.13
pER349	0.18 ± 0.06	1.40 ± 0.03

All values given are mean ± standard deviation from at least three separate determinations.

As noted in the Introduction, the HBD peptide forms dimers in solution. By taking advantage of the fact that we have two forms of significantly differing size (i.e. the fusion protein and cleaved HBD peptide) for each protein, we can measure the rate of dissociation of the dimers (Figure 12). We have previously shown (9) that ligand binding alters the kinetics of dimer dissociation.

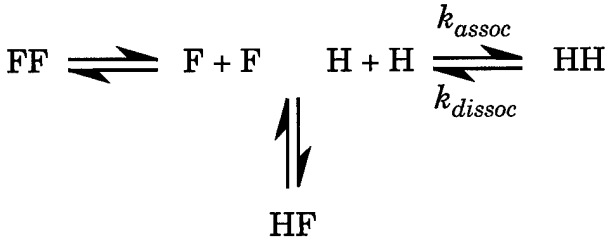

Figure 12. The dimer rearrangement reaction. FF, fusion protein homodimer; HH, HBD homodimer, HF, heterodimer. Since dimer formation is mediated exclusively by the HBD portion of the fusion protein, and since the HBD sequence present in the fusion protein and HBD are identical in each experiment, it is likely that the k_{dissoc}, is similar for both fusion protein and HBD homodimers and for the heterodimer; if not, the measured value will be that of the slower of the two homodimer dissociation rates. Additional experiments, using excess fusion protein suggest that the rate of HBD dissociation is lower than that of the other species in solution.

Dimer dissociation kinetics in the presence and absence of ligand was also tested for the peptides listed in Table 3. The procedure is described in the Methods section; briefly, the fusion protein and HBD peptide were subjected to gel filtration chromatography at various times after mixing. A plot of homodimer concentration (determined from peak area) *versus* time after mixing fits a first order exponential (Figure 13).

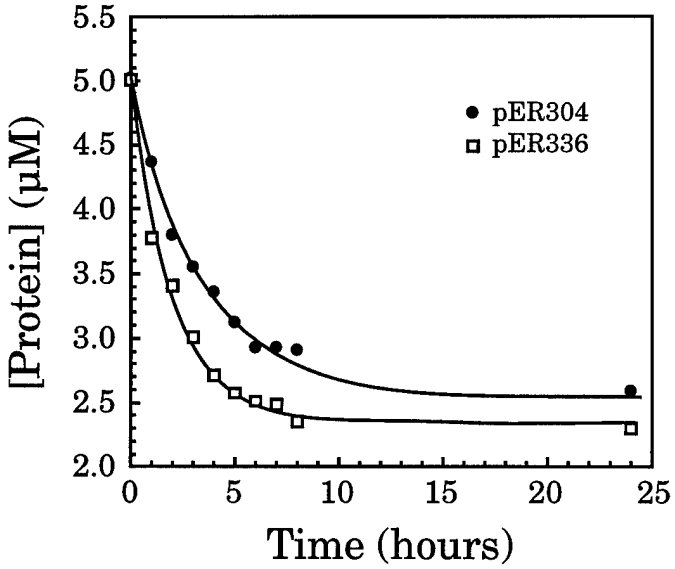

Figure 13. Kinetics of homodimer dissociation. The homodimer concentration (determined from the peak area corrected for protein extinction coefficient) was plotted against time after mixing for pER304 and pER336. For clarity, only the fusion protein homodimer concentration is shown; the HBD peptide homodimer yielded similar kinetics. The curves represent non-linear regression fits to an exponential rate equation.

The results from these experiments are summarized in Table 4. In the absence of ligand, most of the constructs have dissociation $t_{1/2}$ of 1-2 hours; the values were

all compared to pER304, which has the closest to wild-type sequence. The various mutations generally decrease the $t_{1/2}$. The presence of ligand increases the $t_{1/2}$ of dissociation, although for most constructs, these increases are smaller than that for pER304. The exception is pER349; this peptide has a longer $t_{1/2}$ than pER304, but binding of ligand has no effect on its rate of dissociation. These data also suggest that the composition of the N-terminus of the HBD affects the dimer interaction.

Table 4
Dimer Dissociation Kinetics for HBD N-terminal Mutant Peptides

Protein	Ligand	$t_{1/2}$ (hours)	Fold-change
pER304	None	2.8 ± 0.7	--
	Estradiol	12.6 ± 1.5	4.5 *vs.* no ligand
	4-Hydroxytamoxifen	22.6 ± 3.1	8.1 *vs.* no ligand
pER336	None	1.2 ± 0.3	0.4 *vs.* pER304
	Estradiol	3.7 ± 0.6	3.0 *vs.* no ligand
	4-Hydroxytamoxifen	5.3± 1.4	4.4 *vs.* no ligand
pER348	None	2.1 ± 0.5	0.8 *vs.* pER304
	Estradiol	7.7 ± 0.6	3.7 *vs.* no ligand
	4-Hydroxytamoxifen	6.2 ± 1.1	2.9 *vs.* no ligand
pER330	None	2.2 ± 0.3	0.8 *vs.* pER304
	Estradiol	7.3 ± 1.2	3.4 *vs.* no ligand
	4-Hydroxytamoxifen	11.6 ± 2.1	5.4 *vs.* no ligand
pER335	None	1.4 ± 0.2	0.5 *vs.* pER304
	Estradiol	4.7 ± 0.5	3.3 *vs.* no ligand
	4-Hydroxytamoxifen	6.3± 0.7	4.4 *vs.* no ligand
pER349	None	5.0 ± 2.2	1.8 *vs.* pER304
	Estradiol	6.0 ± 1.0	1.2 *vs.* no ligand
	4-Hydroxytamoxifen	4.8± 2.0	1.0 *vs.* no ligand

All values given are mean ± standard deviation from at least two separate determinations.

The estrogen receptor HBD model predicts that the N-terminus of the HBD is exposed to solvent and does not strongly interact with the core of the protein. This appears to be the case for the RXR crystal structure as well. However, the results presented in this section suggest that the N-terminus of the HBD strongly influences the remainder of the protein. Constructs truncated by 3-5 amino acids, or single charge reversal point mutations result in unstable proteins. In addition, alterations at the N-terminus affect the strength of the dimer interaction. Finally, the results suggests that positively charged residues within the N-terminus are

important for the structure of this segment and its interaction with the rest of the protein.

Effect of Varying C-termini

One possible reason for the observed difficulty in crystallization of the HBD is the protrusion of the C-terminal α-helix from the core of the peptide. It is possible that a decrease in the size of this region of the HBD might alter the behavior of the HBD. An estrogen receptor mutant terminated after amino acid 530 was reported to be stable (30). Plasmids based on pER336 were therefore produced with mutations of HBD positions 530 (designated pER340) and 535 (designated pER350) to stop codons. The effect of these mutations on the estrogen receptor model are shown in Figure 14.

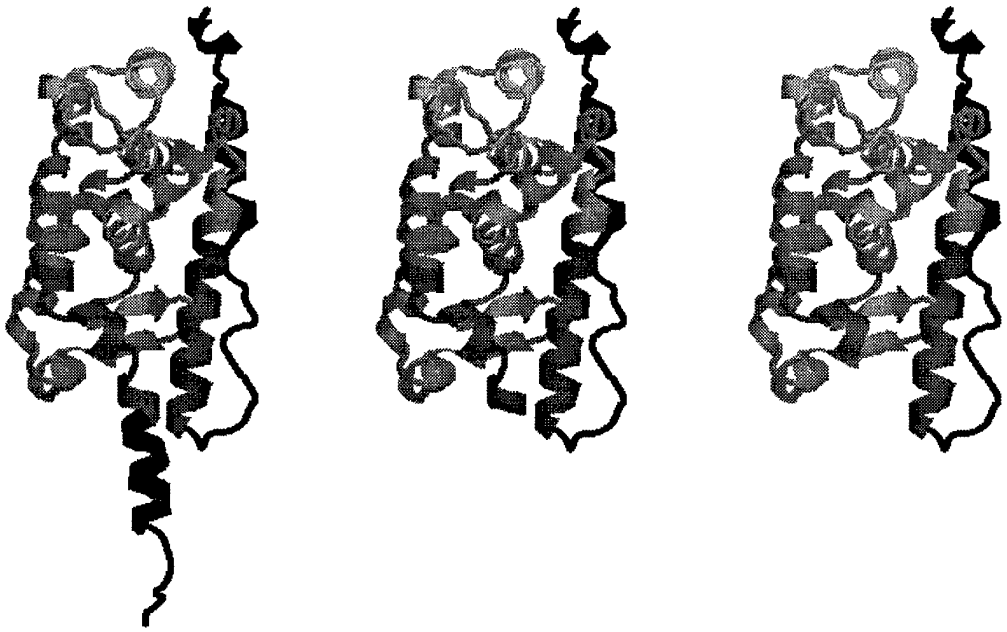

Figure 14. The estrogen receptor model ending at 551 (left), 534 (center), and 529 (right).

The protein from both of these C-terminal shortened constructs were found to be unstable. In contrast, pER334, which also ends at position 534, but is based on pER330 rather than pER336 (see Figure 11), is more stable, but exhibited inhibited cleavage with hydroxylamine. These data suggest that the mutations at both the N- and C-termini affect the overall fold of the HBD.

Tryptophan Mutation Experiments

We have shown that the HBD peptide exhibits fluorescence, and that this

fluorescence is quenched by 4-hydroxytamoxifen (see original application). We proposed to examine the effect of tryptophan mutations on the properties of the protein and on the effects of ligand binding. Figure 2 shows the locations of the Trp residues (positions 360, 383, and 393). Trp-360 and Trp-383 are conserved in RXR-α; all of the Trp residues are conserved in all of the estrogen receptor sequences known, including the estrogen receptor-β, and among all of the human steroid receptors.

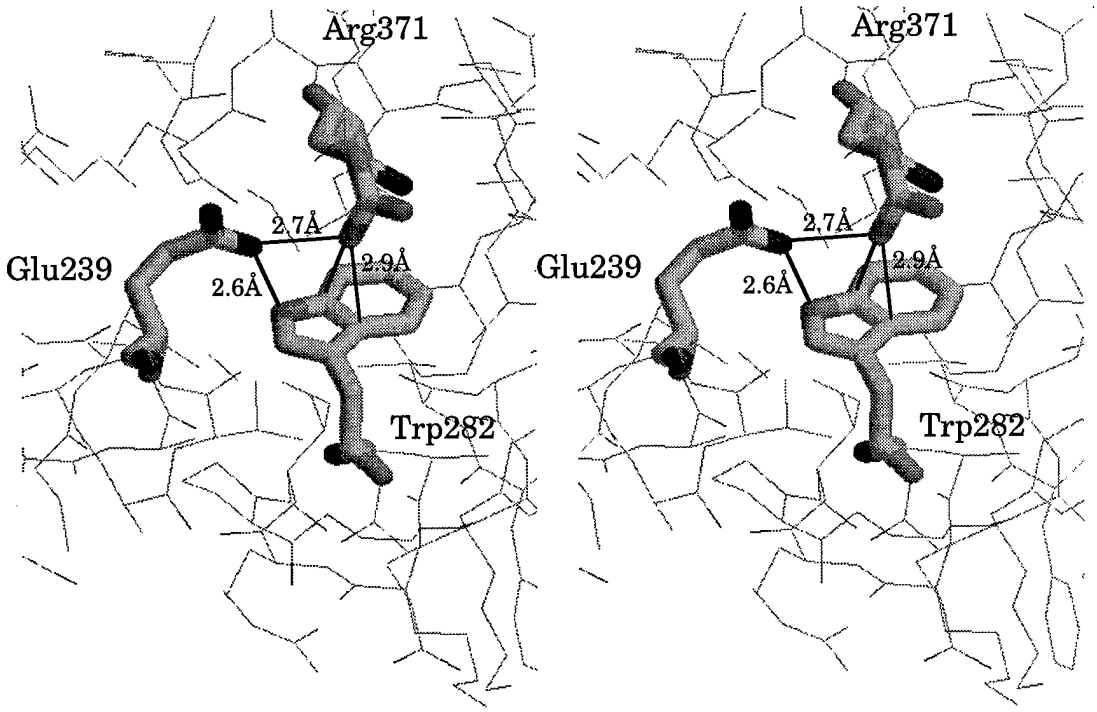

Figure 15. Stereoview of the region around Trp282 of the RXR.

Mutation of the Trp to Phe was chosen since Phe has negligible fluorescence and, while small is similar to Trp in hydrophobicity. The single mutants, W383F and W393F, produced stable proteins; however, W360F did not. While it was possible to measure estradiol binding for the W360F fusion protein (K_d = ~1.5 nM, suggesting somewhat reduced affinity for estradiol), the protein denatured during the purification procedure. Mutation of Trp-360 to Tyr appeared to result in a more stable fusion protein, with a higher affinity for estradiol. However, the W360Y mutant also denatured during the purification procedure. Addition of estradiol during the purification procedure in an attempt to stabilize the fusion protein had only limited effect.

The reason for the instability of the Trp360 mutants is not entirely clear. While most of the receptor proteins have tryptophan at this position, the corresponding residue in RAR-γ is a phenylalanine. Examination of the RXR structure suggests one possible explanation. The corresponding Trp282 is completely buried, and appears to be interacting with the buried salt bridges between Glu239 and Arg371; Glu239 is in close proximity to the indole nitrogen of Trp282, and one of the

guanidinyl nitrogens of Arg371 is interacting with the Trp π-cloud. It is therefore possible that the corresponding residues of the estrogen receptor HBD, Glu 323 and Lys449 require a similar interaction, and neither tyrosine nor phenylalanine fully stabilize the local structure.

Fluorescence is strongly dependent on local environment. The fact that the antagonist ligand 4-hydroxytamoxifen quenches the tryptophan fluorescence in the HBD while the agonist ligand estradiol does not, suggests that fluorescence of the native tryptophan residues may offer information as to the source of the differences in the conformational changes induced by agonist and antagonist. However, the presence of three tryptophan residues within the estrogen receptor HBD complicates interpretation of the data. The ER HBD model predicts that Trp383 and Trp393 are at least partially exposed on the surface of the protein (with Trp383 near the entrance to the ligand binding site), while Trp360 is predicted to be buried (Figure 16). It was therefore of interest to mutate these residues singly and in pairs to non-fluorescent residues. Fluorescence would then be measured for these mutant peptides alone, in the presence of ligand, and in the presence of quenching agents. This will allow further tests of the model and may lend insight into the differences in conformational changes induced by the binding of different classes of ligands.

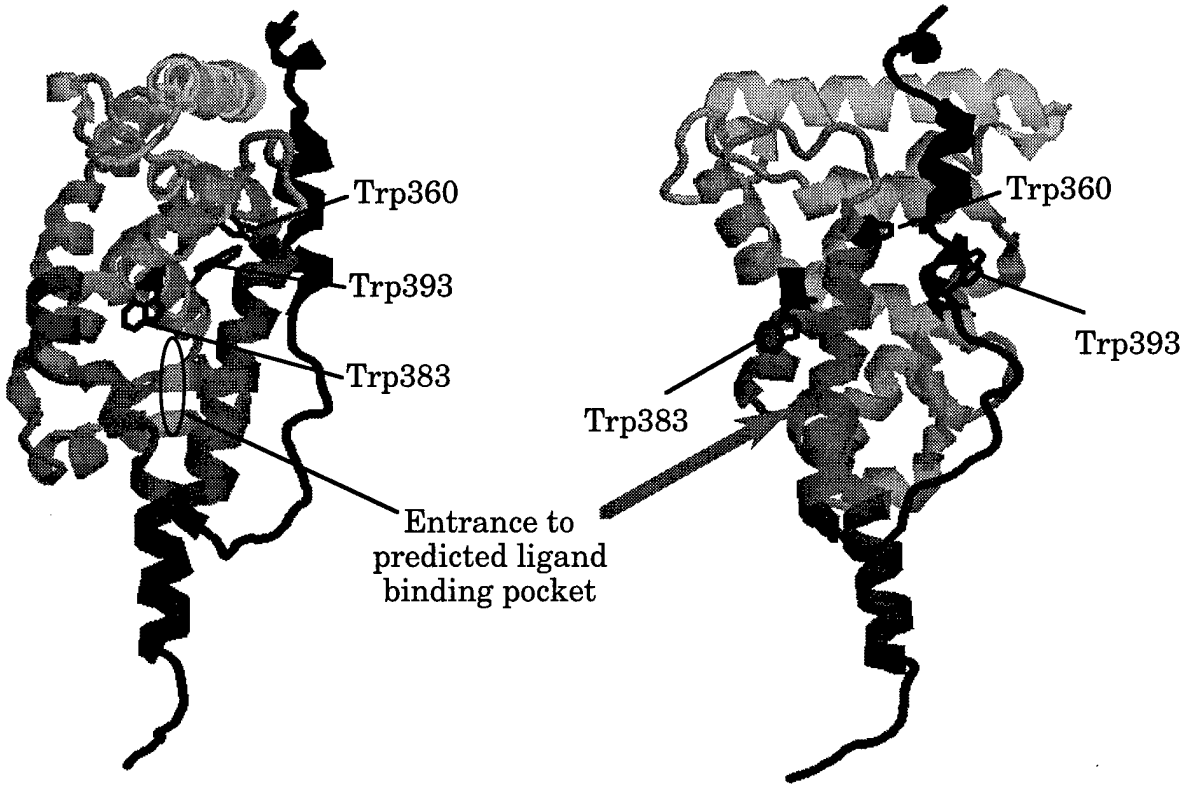

Figure 16. Predicted location of tryptophan residues in the estrogen receptor HBD model. The cartoon on the right is turned roughly 90° relative to the one on the left; the ligand is predicted to enter from the left.

REFERENCES

1. Evans, R.M. (1988)*Science* **240**, 889-895
2. Tsai, M.J. and O'Malley, B.W. (1994) *Annu. Rev. Biochem.* **63**, 451-486
3. Eilers, M., Picard, D., Yamamoto, K.R., and Bishop, J.M. (1989) *Nature* **340**, 66-68
4. Bourguet, W., Ruff, M., Chambon, P., Gronemeyer, H., and Moras, D. (1995) *Nature* **375**, 377-382
5. Renaud, J.P., Rochel, N., Ruff, M., Vivat, V., Chambon, P., Gronemeyer, H., and Moras, D. (1995) *Nature* **378**, 681-689
6. Wagner, R.L., Apriletti, J.W., McGrath, M.E., West, B., Baxter, J.D., and Fletterick, R.J. (1995) *Nature* **378**, 690-697
7. Danielian, P.S., White, R., Lees, J.A., and Parker, M.G. (1992) *EMBO J.* **11**, 1025-1033
8. Wurtz, J.M., Bourguet, W., Renaud, J.P., Vivat, V., Chambon, P., Moras, D., and Gronemeyer, H. (1996) *Nature Struct. Biol.* **3**, 87-94
9. Brandt, M.E. and Vickery, L.E. (1997) *J. Biol. Chem.* **272**: 4843-4849
10. Kuiper, G.G., Enmark, E., Pelto-Huikko, M., Nilsson, S., and Gustafsson J.A. (1996) *Proc. Natl. Acad. Sci.* **93**, 5925-5930
11. Mosselman, S., Polman, J. and Dijkema, R. (1996) *FEBS Lett.* **392**, 49-53
12. Seielstad, D.A., Carlson, K.E., Katzenellenbogen, J.A., Kushner, P.J., and Greene, G.L. (1995) *Mol. Endocrinol.* **9**, 647-658
13. Sambrook, J., Fritsch, E.F., and Maniatis, T. (1989) *Molecular Cloning: A Laboratory Manual* 2nd Ed. Cold Spring Harbor Laboratory Press, Cold Spring Harbor, New York
14. Kumar, V., Green, S., Staub, A., and Chambon, P. (1986) *EMBO J.* **5**, 2231-2236
15. Tora, L., Mullick, A., Metzger, D., Ponglikitmongkol, M., Park, I., and Chambon, P. (1989) *EMBO J.* **8**, 1981-1986
16. Nelson, R.M. and Long, G.L. (1989) *Anal. Biochem.* **180**, 147-151
17. Bornstein, P., and Balian, G. (1977) *Meth. Enzymol.* **47**, 132-45
18. Deng, W.P., and Nickoloff, J.A. (1992) *Anal. Biochem.* **200**, 81-8
19. Gill, S.C., and von Hippel, P.H. (1989) *Anal. Biochem.* **182**, 319-326
20. Mach, H., Middaugh, C.R., and Lewis, R.V. (1992) *Anal. Biochem.* **200**, 74-80
21. Lowry, O.H., Rosebrough, N.J., Farr, A.L., and Randall, R.J. (1951) *J. Biol. Chem.* **193**, 265-270
22. Bradford, M.M. (1976) *Anal. Biochem.* **72**, 248-254
23. Andrade, M.A., Chacón, P., Merelo, J.J., and Morán, F. (1993) *Prot. Eng.* **6**, 383-390
24. Scatchard, G. (1949) *Ann. N.Y. Acad. Sci.* **51**, 660-672
25. Hill, A.V. (1913) *Biochem. J.* **7**, 471

26. Peitsch, M. C. (1995) *Bio/Technology* **13**, 658-660
27. Peitsch, M. C. (1996) *Biochem. Soc. Trans.* **24**, 274-279
28. Peitsch, M. C. and Jongeneel, C. V. (1993) *Int. Immunol.* **5**, 233-238
29. Harlow, K.W., Smith, D.N., Katzenellenbogen, J.A., Greene, G.L., and Katzenellenbogen, B.S. *J. Biol. Chem.* **264**, 17476-17485
30. Wrenn, C.K. and Katzenellenbogen, B.S. *J. Biol. Chem.* **268**, 24089-24098

28. Sasson, S. and Notides, A.C. (1988) *Mol. Endocrinol.* **2**, 307-312
29. Kumar, V. and Chambon, P. (1988) *Cell* **55**, 145-156
30. Notides, A.C., Lerner, N., and Hamilton, D.E. (1981) *Proc. Natl. Acad. Sci. USA* **78**, 4926-4930
31. Obourn, J.D., Koszewski, N.J., and Notides, A.C. (1993) *Biochemistry* **32**, 6229-6236
32. Lees, J.A., Fawell, S.E., White, R., and Parker, M.G. (1990) *Mol. Cell. Biol.* **10**, 5529-5531
33. Schwabe, J.W.R., Neuhaus, D., and Rhodes, D. (1990) *Nature* **348**, 458-461
34. Schwabe, J.W.R., Chapman, L., Finch, J.T., and Rhodes, D. (1993) *Cell* **75**, 567-578
35. Schwartz, J.A. and Skafar, D.F. (1994) *Biochemistry* **33**, 13267-13273

Appendix
Partial List of Plasmids Constructed

Plasmid	Insert Properties			Comments
	Start	End	Mutation	
pER08	301	551	None	Not designed to be hydroxylamine cleavable.
pER304	Gly+ 300	551	None	Somewhat heterogeneous cleavage by hydroxylamine K_d = 0.25±0.14 nM dissociation $t_{1/2}$ = 2.4 ± 0.4 hr
pER336	Gly+ 300	551	S305E	Homogeneous cleavage K_d = 0.17±0.06 nM dissociation $t_{1/2}$ = 1.2 ± 0.3 hr
pER348	Gly+ 300	551	N304D, S305E	Homogeneous cleavage K_d = 0.17±0.06 nM dissociation $t_{1/2}$ = 2.1 ± 0.5 hr
pER330	Gly-Arg+ 305	551	None	Homogeneous cleavage K_d = 0.20±0.04 nM dissociation $t_{1/2}$ = 2.2 ± 0.3 hr
pER335	Gly+ 306	551	None	Actual insert begins at estrogen receptor codon 300; contains S305G mutation to improve cleavage; Somewhat heterogeneous cleavage by hydroxylamine (additional cleavage site within MBP, in spite of mutation of MBP Asn-368) K_d = 0.19±0.08 dissociation $t_{1/2}$ = 1.4 ± 0.2 hr
pER337	Gly-Arg+ 315	551	None	Unstable; fusion protein binds estradiol, but rapidly loses activity during purification.
pER331	Gly+ 306	551	None	Actual insert begins at estrogen receptor codon 279; contains S305G mutation to improve cleavage; Somewhat heterogeneous cleavage by hydroxylamine (additional cleavage site within MBP)
pER333	Gly+ 306	551	None	Actual insert begins at estrogen receptor codon 300; contains S305G mutation to improve cleavage; Somewhat heterogeneous cleavage by hydroxylamine (additional cleavage site within MBP)
pER349	Gly-Arg+ 310	551	None	Somewhat unstable. K_d = 0.18±0.06 nM dissociation $t_{1/2}$ = 5.0 ± 2.2 hr; not changed by ligand binding.
pER03	301	567	None	Not designed to be hydroxylamine cleavable.

pER05	279	595		Not designed to be hydroxylamine cleavable. Poor expression; proteolytic degradation occurs within cells.
pER332	Gly-Arg+305	595	None	Poor expression; proteolytic degradation occurs within cells.
pER334	Gly-Arg+305	534	None	Heterogeneous cleavage Fusion protein K_d = 0.14
pER340	Gly+300	529	S305E	Unstable
pER350	Gly+300	534	S305E	Unstable
pER306	Gly+300	551	W360F	Unstable Fusion protein K_d = 1.56±0.21
pER316	Gly+300	551	W360Y	Fusion protein K_d = 0.52±0.01 Insufficiently stable for purification
pER307	Gly+300	551	W383F	K_d = 0.2 nM
pER308	Gly+300	551	W393F	K_d = 0.2 nM
pER310	Gly+300	551	W360F, W383F	Constructed and sequenced (expected to be unstable).
pER311	Gly+300	551	W360F, W383F	Constructed and sequenced (expected to be unstable).
pER312	Gly+300	551	W383F, W393F	K_d = 0.1 nM
pER313	Gly+300	551	W360F, W383F, W393F	Unstable
pER318	Gly+300	551	W360Y, W383F, W393F	Constructed and sequenced.
pER314	Gly+300	551	R503A	Unstable
pER315	Gly+300	551	L507R	Low level of protein expression (unstable?) Fusion protein K_d = 0.6
pER341	Gly+300	551	S305E, L509R	Constructed and sequenced.
pER317	Gly+300	551	S305E, C447W	Fusion protein K_d = ~1.6 (low but detectable activity in screening assay)
pER323	Gly+300	551	S305E, C381S	Constructed and sequenced.

pER305	Gly+ 300	551	G366S	Fusion protein K_d = 0.45
pER11	279	567	A361V	Fusion protein K_d = 0.32
pER04	Gly+ 300	567	S433P	Estradiol binding detectable but very low (~100x below active constructs in screening assay).
pER370	Gly+ 300	551	Δ483-514	Extremely low activity in screening assay.
pER371	Gly+ 300	551	Δ474-505	Extremely low activity in screening assay.